The rigorous application of cavity expansion data

L'application rigoureuse des données d'expansion de cavité

John Hughes [1], Robert Whittle[2]

[1]*Retired, formerly owner of Hughes Insitu Engineering, Canada*
[2]*Cambridge Insitu Ltd, England. Contact: Robert @Cambridge-Insitu.com*

ABSTRACT

The first commercially available pressuremeter test was developed by Louis Ménard in the late 1950s and was very successful in certain circumstances as a tool for foundation design. The Ménard method is a combination of pressuremeter specific measurements and empirical correlations. As early as 1961 it was realised that the same field data could be interpreted using basic mechanics, so that the test can be expressed as soil parameters for strength and limit pressure without the need for empiricism. Furthermore, if the resolution of the equipment was increased, it was possible to measure the sub-yield response of the material, assuming that probe itself could be introduced into the ground without significant alteration to the initial stress state. The self-boring pressuremeter was developed in the early 1970‘s to achieve these goals. There have been substantial advances in equipment, techniques and analysis since then, and this paper describes the current situation. The one property of the ground that the high resolution pressuremeter can provide in a repeatable manner without difficulty is shear modulus and the variation of modulus with strain and stress. This ability is now becoming widely acknowledged and is fundamental to the application of pressuremeter data.

RESUME

Le premier essai pressiométrique commercialisé a été développé par Louis Ménard à la fin des années 1950 et s'est avéré très efficace dans certaines circonstances comme outil de conception de fondations. La méthode Ménard combine des mesures pressiométriques spécifiques et des corrélations empiriques. Dès 1961, on a réalisé que les mêmes données de terrain pouvaient être interprétées à l'aide de la mécanique de base, permettant ainsi d'exprimer l'essai sous forme de paramètres de résistance et de pression limite du sol sans recours à l'empirisme. De plus, en augmentant la résolution de l'équipement, il était possible de mesurer la réponse sous-seuil de rupture du matériau, à condition que la sonde puisse être introduite dans le sol sans modification significative de l'état de contrainte initial. Le pressiomètre autoforeur a été développé au début des années 1970 pour atteindre ces objectifs. Depuis, des progrès considérables ont été réalisés en matière d'équipement, de techniques et d'analyse, et cet article décrit la situation actuelle. La seule propriété du sol que le pressiomètre haute résolution peut fournir de manière reproductible et sans difficulté est le module de cisaillement et sa variation en fonction de la déformation et de la contrainte. Cette capacité est désormais largement reconnue et est fondamentale pour l’application des données pressiométriques.

Keywords: Resolution; Self boring; Strength; Insitu lateral stress; Shear modulus; Yield

1. Introduction

It is a curiosity that the best-known solution for the cavity expansion test (Gibson & Anderson, 1961) is an adaptation of an earlier solution (Bishop, Hill & Mott, 1945) that precedes by several years the first commercial pressuremeter. The earlier paper solves the problem of a cylindrical punch driven into a ductile material and in particular derives a limit pressure.

Empirically at least, this concept had been appreciated in the maritime world for at least 200 years. The cannon (Fig.1) is a physical representation of a cavity expansion, with dimensions and the charge arranged to remain within the elastic range of the material from which it is constructed. Exceed the elastic range and the cannon may explode. Making the barrel thicker will not allow a more powerful charge to be used. This can only be done by using stiffer material, iron or steel instead of bronze.

1.1. The Menard system

Gibson & Anderson illustrate their solution using data obtained from a Ménard pressuremeter test (Fig. 3). This device had been in commercial use since about 1957. Louis Ménard (1933-1978) was a brilliant French engineer who had developed a pre-bored expanding pressuremeter system. His “Pressuremeter” (MPM) used a rubber membrane to load the borehole wall (Fig. 2) and

measured three parameters – a limit pressure, a creep pressure and a modulus. For the time it showed an innovative appreciation of the behaviour of soil.

Figure 1. 19C cannon outside Ely Cathedral

What Ménard observed is that the displacement/ pressure curve was distinctly non-linear and the pressure tended to a steady state limit. Hence, working backwards, there was a relationship between this limit and the strength of the soil.

The second observation was that after contacting the cavity wall the initial part of the pressure expansion curve

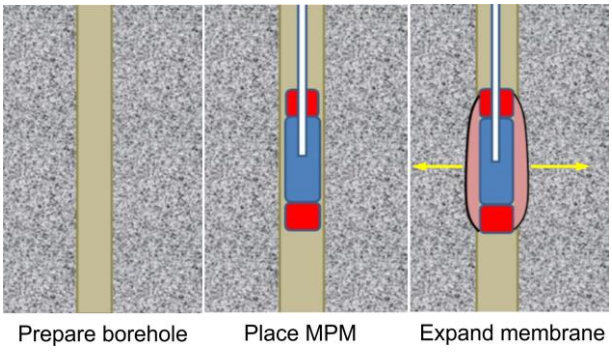

Figure 2. The Ménard system

had an extended linear portion. The slope of this gave a modulus related to the stiffness of the ground.

The third observation was "creep pressure." As a consequence of the method of applying pressure and the need to write the values by hand, he observed that there was a pattern in the amount of movement (creep) between successive steps of pressure (Fig. 3)

Although there have been some refinements to the equipment, this remains the basis of the Ménard method. It is an empirical approach with some analytical background. The probe itself has no active parts. The parameters produced are specific to the method and are not fundamental soil properties. Nevertheless it has been shown by many that these parameters can be related to the field performance of simple structures.

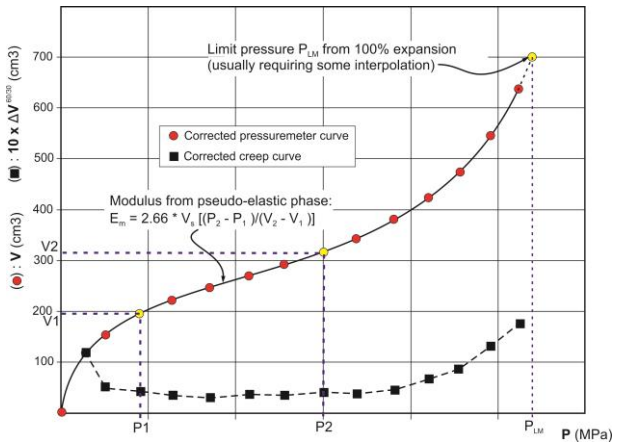

Figure 3. Annotated MPM curve

1.2. Self boring

The best known self-boring system was developed at Cambridge University (CU) in the early 1970s by John Hughes and his supervisor Peter Wroth. The initial intention was to use the self-boring method to place a sensitive load cell in the ground. As the external pressure acted on the cell, a feed back system raised the internal pressure to prevent the load cell deflecting. When equilibrium was achieved, this gave the insitu lateral stress, assuming perfect placement. Fig. 4 is a later example of this procedure, Fig. 5 shows the probe and its

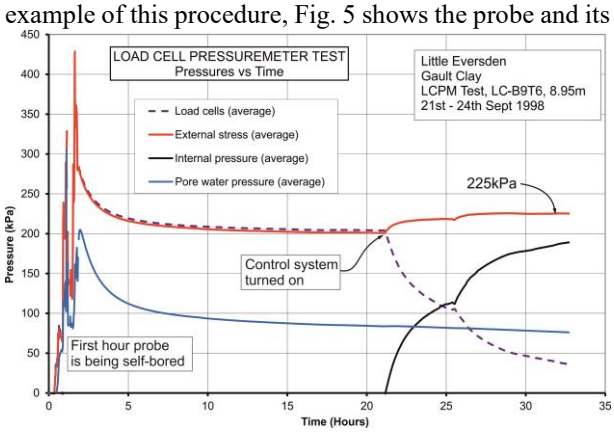

Figure 4. LCPM test in very stiff clay

control system, Fig. 6 is a schematic of one section showing the three types of transducer employed.

Due to the time taken to perform the test, the Load Cell Pressuremeter (LCPM) has been used primarily for research. Fig. 4 shows the system output whilst it is being drilled in (first hour), allowed to settle (1 to 21 hours) then responding as the control system is turned on and raises the internal pressure. The derived external stress is the sum of the internal pressure and any residual output from the load cell. Assuming that this combined total represents the insitu lateral stress σ_{ho}, the coefficient of earth pressure at rest, k_0, is 1.2 for this example.

Hughes then considered a self-boring expansion pressuremeter with the potential for obtaining the full stress-strain curve for the material in addition to the insitu stress. Adapting an MPM was considered but rejected, partly due to the comparatively low resolution of the MPM system. To put this in context, for a typical soil, all

the sub-yield information is contained in the first 1% shear strain of the expansion and so would barely register

Figure 5. Six axis self boring LCPM and controller

in an MPM test, where 1% is a change of 7cm^3 for the original MPM.

CU had developed a system of taking x-ray photographs of soil samples loaded with strategically placed lead shot. This technique was used to prove the potential of the self-boring method. It also proved that radial displacement at the centre of an expanding membrane was insensitive to the membrane length and therefore representative of a cylindrical cavity expansion. Fig. 7 is an example (overdrawn, as the original photograph does not reproduce well).

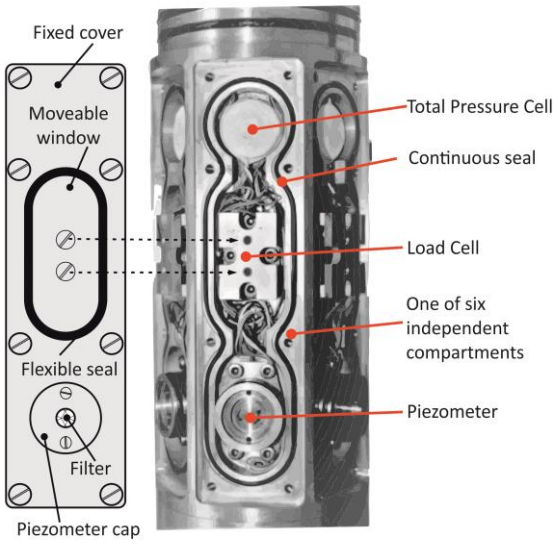

Figure 6. Sketch of one section of the LCPM

The Cambridge Self Boring Pressuremeter (SBP) is built around a 51mm diameter stainless steel tube with a 6.4 mm wall thickness. It has been manufactured since

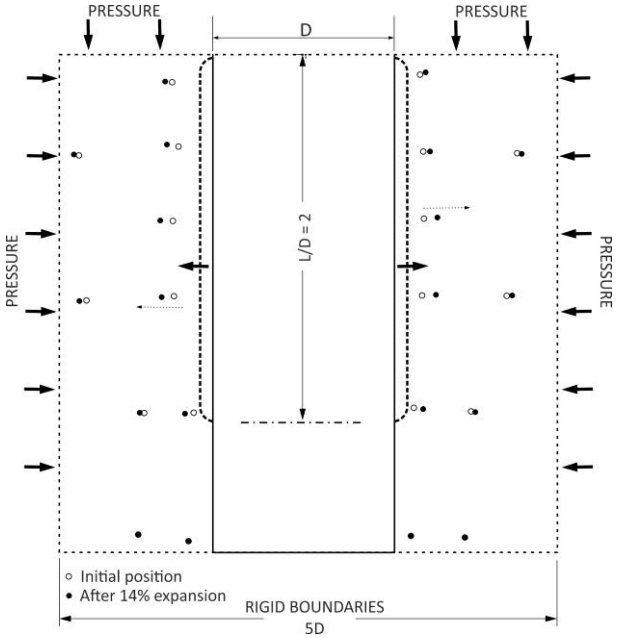

Figure 7. Enhanced radiographic image of cavity expansion experiment

1975 by Cambridge Insitu Ltd (CIL). Although there have been substantial changes the device retains many of the original features. It reads total pressure, pore water pressure, and radial displacement at six points equally spaced in the same plane. All measurements are made in the probe itself and since the early 1990s all signal conditioning including analogue to digital conversion is carried out within the body of the probe. In its original form the diameter was arranged to be the same (within a few micrometres) from the foot of the cutting shoe to the top end of the expanding section.

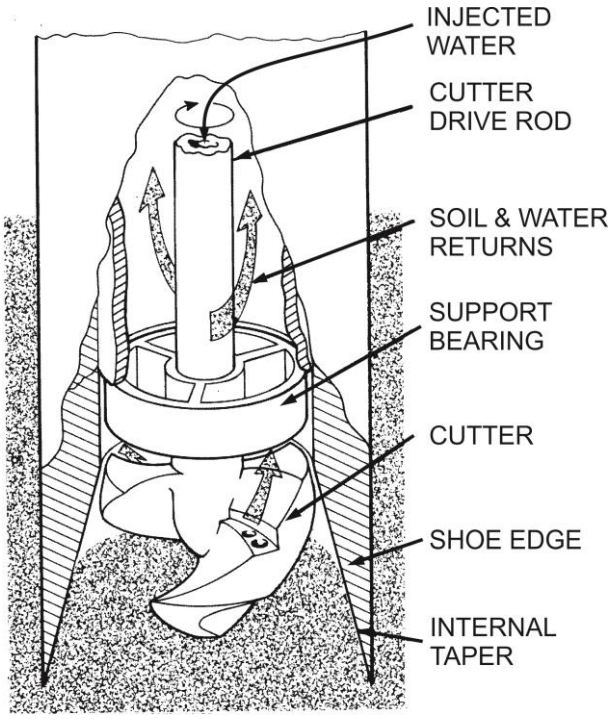

Figure 8. The original self boring head

The self boring head is sketched in Fig.8. It uses a two part drill string. The outer part continues the 51mm diameter of the body of the probe. It carries downthrust but not rotation. The inner cutter drive rod (CDR) passes through the centre. It sees rotation but only mild torque, and also acts as a water line. The downthrust forces the internally tapered sharp shoe edge into the material. As soil enters the shoe space the rotating cutter breaks it down and the injected water transports the cuttings back to the surface. The return path is the annulus between the CDR and the inner wall of the outer tube. No water passes around the outside of the instrument.

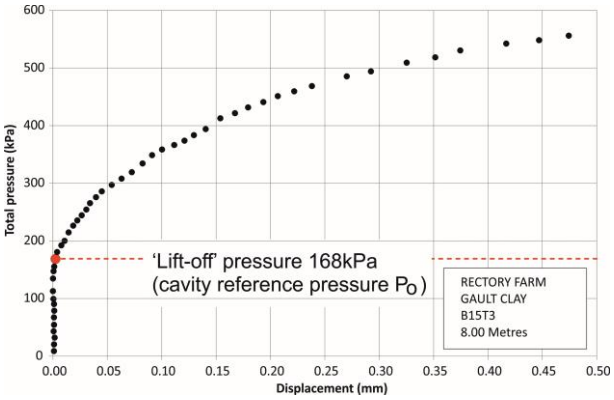

Figure 9. The first 0.5mm of an SBP test in stiff clay

In the soils that it was designed for, soft clays and loose sands, the system works extraordinarily well. In practice it is frequently used in stiff clays and dense sands, and the current version of the SBP is necessarily more robust than the original tool. In general the system is set-up to use a maximum downthrust equivalent to about 2 tonnes. There are alternative drill heads, including one capable of boring into weak rock. There is also a jetting system for material such as tailings that can be cut with water pressure alone. For this jetting system, rotation is not required and there is no inner rod other than a jetting lance through the centre of the SBP. A good self-bored test is capable of producing a field curve that shows very little obvious disturbance, potentially allowing insitu stress and strength data to be read directly from the measured data, the so-called 'lift-off' pressure (Fig. 9).

The difficulty with data such as Fig. 9 is the implicit assumption that the disturbance caused to the ground is negligible. This is unsafe – disturbance must always be quantified.

A more complete interpretation of the data in Fig. 9 is given in Fig. 10, where the whole curve is used to find the parameter set that best represents what was measured. It is then possible to see that the so -called 'lift-off' value, the stress at which the cavity starts to expand, is an under-estimate.

In Fig. 9 and Fig. 10, P_0 refers to the cavity reference pressure. It is a matter of engineering judgement whether this is also representative of the insitu lateral stress, σ_{ho}.

The approach used to reconstruct the pressuremeter field curve in Fig. 10 is described in more detail later. However note that the value for P_0 in Fig. 10 and external stress in Fig. 4 are in good agreement. The two borehole locations are only a few metres apart at the former Rectory Farm test site.

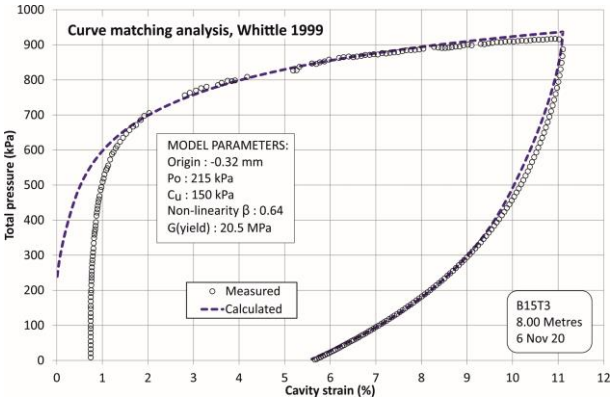

Figure 10. Reconstructing the SBP test

A significant component of the development of the SBP and the family of pressuremeters often referred to as 'Cambridge' is the realization that disturbance is always present. The test method is designed to quantify and erase it, allowing the undisturbed sub-yield response of the ground to be discovered. Every co-ordinate of pressure-displacement in the test is decided by the same set of soil parameters for strength, stiffness and the initial stress state. Viewed at in this way, it is easier to identify the elusive σ_{ho} from the test as a whole rather than from direct observation.

It has taken many years to develop the current testing methods. It required the arrival of cheap computing power and rapid sampling rates. The methods continue to evolve.

This paper focuses on the development of the undrained solution for the self-bored test, because at the present time this is the most complete combination of analysis and synthesis. The drained case is presented more briefly.

2. The stress-strain curve (undrained case)

The pressuremeter field curve is the integration of the stress-strain response of the ground. Hence differentiating the field curve at any point gives the current mobilized stress. For the undrained case, Palmer (1972) relates shear stress τ to total pressure P and current cavity strain ε_c as follows:

$$\tau = \varepsilon_c(\mathrm{dP}/\mathrm{d}\varepsilon_c) \qquad (1)$$

This can be solved graphically, and prior to easy access to computers, was the solution of choice (Fig. 11).

Eq. (1) is extremely powerful. It makes no assumptions about the form of the stress-strain curve. As a means of finding the current shear stress it is applicable to all parts of the pressuremeter curve provided that the relevant displacement origin for a particular event can be identified. In the example it is applied to the loading phase. It can also be applied to an unload/reload cycle or the final cavity unloading phase, assuming that the local origin when the direction of loading changes is defined. If the origin is inaccurate, so that strain is miscalculated, then the procedure will produce misleading shear stress

values, but this is an effect that diminishes with distance from the assumed origin.

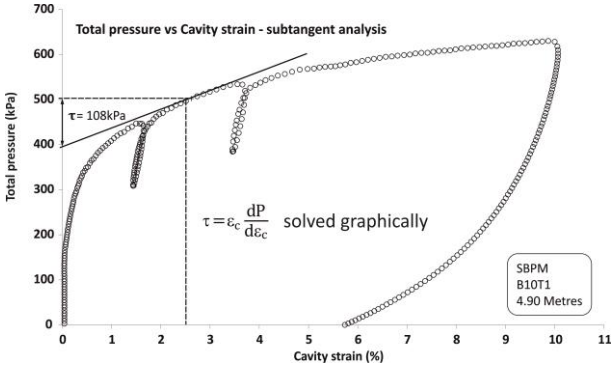

Figure 11. The sub-tangent analysis for shear stress

Palmer (1972) is a numerical solution. Gibson & Anderson (1961) is a closed form solution. It assumes the shape of the stress-strain response and solves the boundary problem (Eq. (2)). The assumption is that the ground deforms in a linear elastic manner until the shear stress at failure is achieved. Thereafter the response is perfectly plastic.

This is an unrealistic description of soil behaviour and the next level of sophistication is to propose that below yield the ground response is non-linear, with the assumption of perfect plasticity retained (Fig. 12). The undrained solution for this case is given by Bolton & Whittle (1999). Refer to Eq. (3).

$$P_c = P_o + c_u[1 - \log_e(c_u/G) + \log_e(\Delta A/A)] \quad (2)$$

$$P_c = P_o + c_u[1/\beta - \log_e(c_u/G_{ye}) + \log_e(\Delta A/A)] \quad (3)$$

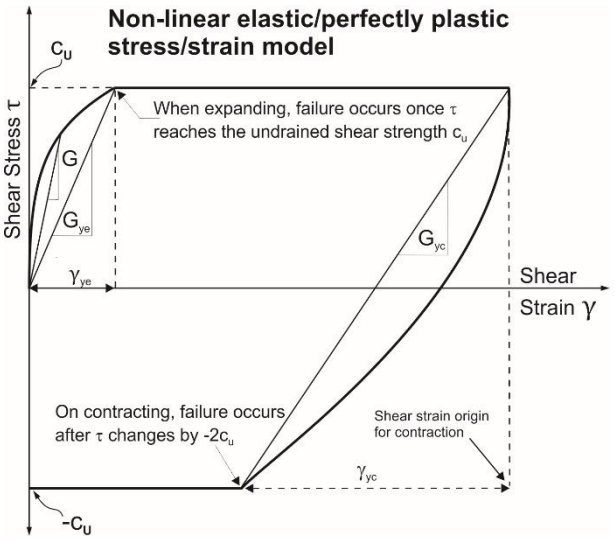

Figure 12. Assumed stress-strain response

All terms are defined in Table 1. Eq. (3) has been used to create the modelled data in Fig. 10. Both eq. (2) and eq. (3) can be applied graphically to find the limit pressure P_L of the ground when $\Delta A/A = 1$.

Houlsby & Withers (1988) and Jefferies (1988) both give solutions for an undrained linear elastic/perfectly plastic cavity contraction. The non-linear version of these is given by Whittle (1999) and the plastic phase can be written as follows:

$$P_c = P_{mx} - 2c_u/\beta - 2c_u \log_e[y_{cc}/y_{yc}] \quad (4)$$

The exponent of non-linearity β appears in both equations (3) and (4). Its derivation and how it is obtained is now described.

3. Shear modulus

A compelling argument for the high resolution pressuremeter test (regardless of the insertion method or probe type) is the ability to determine the sub-yield response of the ground in a repeatable manner. This is done using small cycles of unloading and reloading. Fig. 11 is an example of an SBP test in clay and Fig. 13 is an example of an over-water pre-bored test in silty sand.

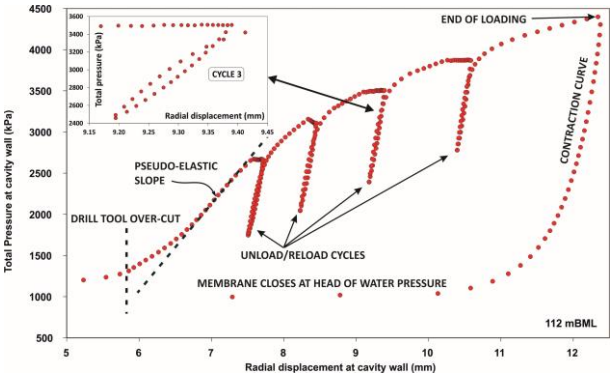

Figure 13. A pre-bored test in silty sand (over-water)

This test has 4 cycles taken whilst the cavity is expanding, each very similar to the others. Early argument for this technique assumed a linear response but as the inset shows, the unload/reload event has a hysteretic appearance. This is due to the non-linear nature of soil stiffness at strains below the yield condition.

For comparison purposes the pseudo-elastic response, directly equivalent to the part of the MPM curve used to calculate E_M in Fig. 3, is also shown. It is apparent that the initial slope is dominated by the consequences of pocket preparation with the subsequent relaxation, and is unrepresentative of the true shear stiffness.

Fig. 14 is an annotated example of a real cycle with some of these features brought out.

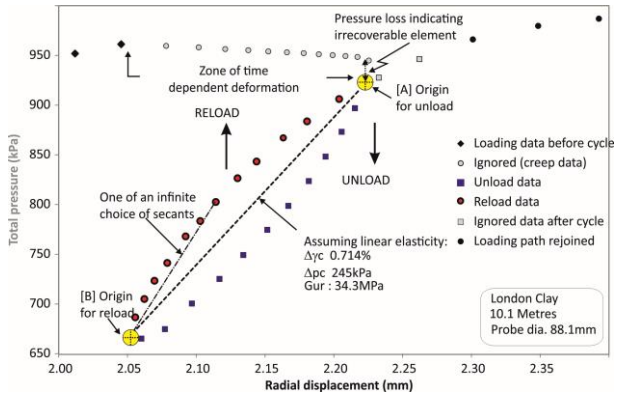

Figure 14. Annotated unload/reload cycle

Fig . 14 shows that the unloading and reloading data are equivalent to each other. Because the unloading is affected by creep from the preceding expansion, origin [A] is less certain than origin [B], where the cycle turns around. If secants are drawn from origin [B] to touch the

reloading envelope then each would give a different strain dependent value for shear modulus. It is straightforward to calculate the shear strain and the change of radial stress for each of the data points in the reloading path. Bolton & Whittle (1999) show that this response is accurately represented by a power curve (Fig. 15).

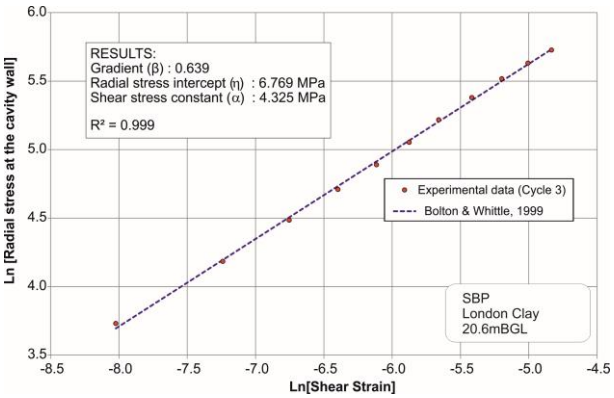

Figure 15. Deriving the non-linear parameters

The data are plotted in radial stress – shear strain space and need to be converted to shear stress-shear strain values. This can be done by adapting the Palmer (1972) result given by equ. (1):

$$\tau = \gamma(dP/d\gamma) \quad (5)$$

The power law result is:

$$P = \eta\gamma^{\beta} \quad (6)$$

Hence:

$$\tau = \eta\beta\gamma^{\beta} \quad (7)$$

Bolton and Whittle refer to ηβ as α and call it the shear stress constant. Shear modulus is the derivative of shear stress, so secant shear modulus is given by:

$$G_s = \alpha\gamma^{\beta-1} \quad (8)$$

β takes a value between 0.5 and 1, where 1 is linear elastic.

Fig. 16 shows three cycles from a test in London Clay plotted as stiffness-decay curves:

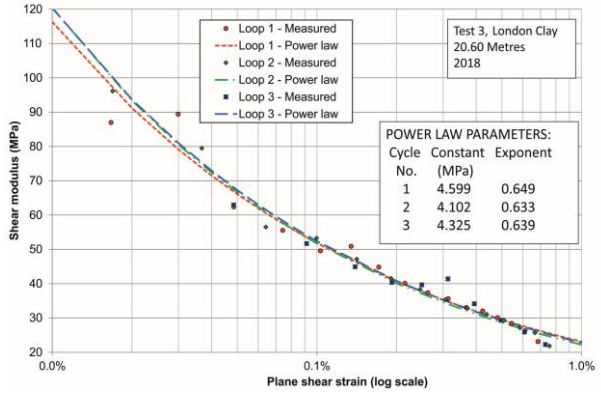

Figure 16. Stiffness decay curves, undrained test

The lines in Fig. 16 are the power law trends plotted between arbitrary shear strains 0.01% and 1%. All cycles give the same response because following undrained yield, the mean effective stress at the cavity wall is constant. The data points come from applying the sub-tangent analysis described by Fig. 11 directly to the data points from the reloading path of each cycle. Directly differentiated experimental data is affected by small measurement uncertainties but the results clearly follow the same trend as the power curves.

There are two limitations for the wider application of shear modulus determined in this way. One is the direction of loading. The ground is sheared horizontally and responds with horizontal movement (assuming a vertical borehole) so the test produces G_{HH} modulus parameters. In an over-consolidated clay these are generally higher than G_{VH} values from other test methods. The second limitation is the vagueness of the very small strain data. This is not a resolution but a control issue. Within a cavity expansion test it is difficult to arrange for miniscule pressure changes when following the unload/reload event. Hence the usual practice is not to quote shear modulus parameters for shear strains smaller than 10^{-4}.

4. Curve modelling

Modelling the experimental data is the process of finding the parameter set that best represents the measured field curve. Potentially there are multiple solutions but the method outlined by Whittle (1999) is constrained by the values for shear strength obtained from the loading and contraction, and the non-linear stiffness parameters α and β. The only uncertainty is the cavity reference pressure, P_0.

In addition to the plastic equations (3) and (4), two further equations describing the sub-yield response are required. For the loading case, the total pressure at the cavity wall is given by:

$$P = P_0 + \left(\frac{\alpha}{\beta}\right)(\gamma)^{\beta} \quad (8)$$

This applies until $P = P_0 + c_u/\beta$.

For the cavity contraction sub-yield response, total pressure at the cavity wall is given by:

$$P = P_{mx} - \left(\frac{\alpha}{\beta}\right)(\gamma)^{\beta} \quad (9)$$

This applies until $P = P_{mx} - 2c_u/\beta$. P_{mx} is the maximum pressure at the cavity wall achieved during the loading phase.

4.1. Undrained model assumptions

- It is an assumption that strength is the same whether loading or unloading.
- Because the start of the contraction is known, shear strength derived from this phase of the test is the best estimate.
- If the loading value for strength does not accord with the unloading value then the strain origin for the expansion is moved left or right until the condition is satisfied.
- Adjustment means a small alteration of the initial cavity radius as a means of compensating for insertion disturbance. For a self bored test with disturbance in the sub-yield range this will be an offset less than ±0.2mm. For a pre-bored test it may be several millimetres.

- Having made the shear strengths agree, the final step is to set P_0 for best fit (Fig. 17). The model is sensitive to quite small variations of P_0.

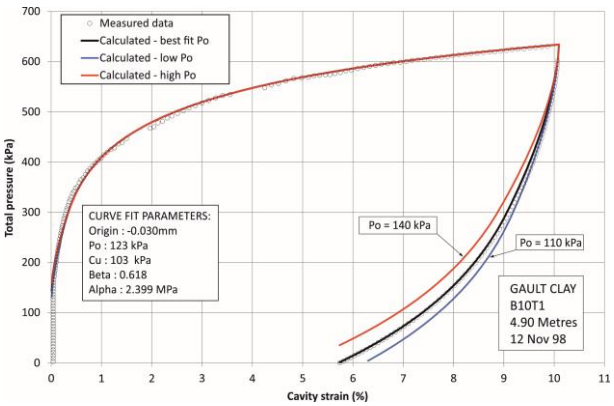

Figure 17. Sensitivity of model to Po variation

4.2. Limitations of the undrained model

The undrained model is straightforward to apply and in principle has minimal uncertainty because the parameters are constrained by the shear modulus results. These are repeatable measurements that apply no matter how far the cavity has been expanded (Fig. 13). A pre-bored or pushed device such as a Full Displacement Pressuremeter (FDPM) will give similar results to the best self-bored test.

However there are undrained tests that the model will not fully describe. Typically, these are:

- Materials that have a true peak in the shear stress-shear strain curve, so not perfectly plastic.
- Normally consolidated clays. Here the problem is that at some point in the cavity contraction the vertical stress becomes the major stress, so deriving strength from the contraction becomes uncertain.

Indicating when the material is not a good match for the model is an essential contribution to the understanding of the ground response.

5. Drained Interpretation

A limited solution for the frictional response of the ground under drained conditions is given by Gibson & Anderson (1961). This assumes constant volume deformation. Hughes et al (1977) is a solution that accounts for volumetric strains and the adopted methodology is the basis for subsequent closed form solutions. Carter et al (1986) includes drained cohesion and elastic strains in the plastic region. Houlsby et al (1987) and Withers et al (1989) give solutions for cavity contraction. Manassero (1988) is a numerical solution for the frictional response of drained cavity expansions and this can be extended to cavity contraction (Whittle & Byrne, 2020).

The closed form solutions assume that the internal angle of friction remains constant, which is approximately the case for an SBP with its limited range.

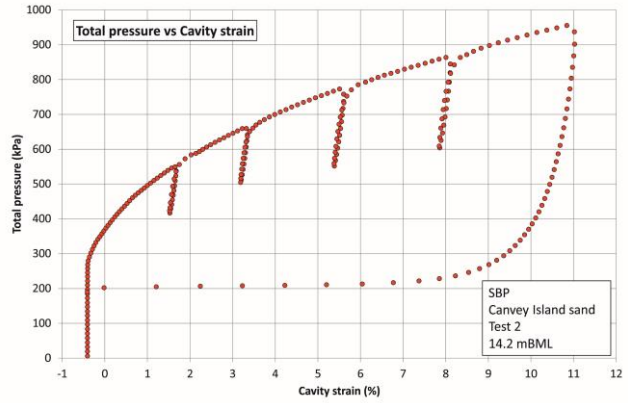

Figure 18. SBP test in medium dense sand

A log-log plot of effective radial stress against cavity strain gives an ultimate slope whose gradient can be converted to friction and dilation angles using Rowe's

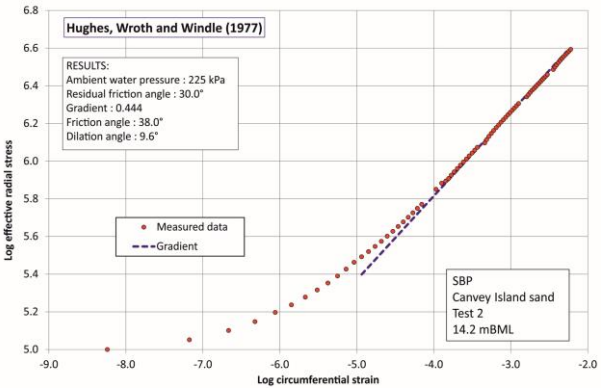

Figure 19. Finding the friction angle

theorem of dilatancy (Fig. 19). This is a reasonable assumption for a cavity expansion in medium to dense sands but the peak behaviour during a cavity contraction is usually not sustained for more than a small strain reduction. Modelling the drained ground response in an analogous manner to the undrained case is therefore less satisfactory.

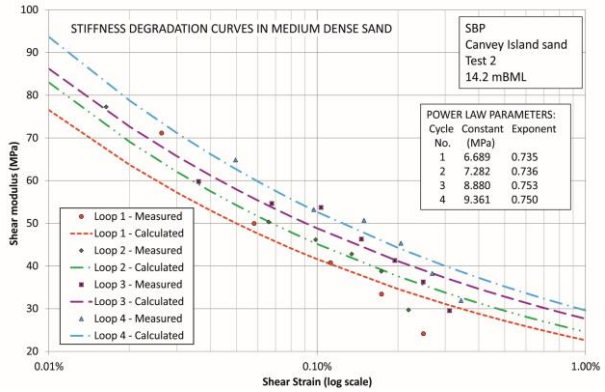

Figure 20. Stiffness degradation with stress dependency

A second difficulty is that constraining the model with high quality stiffness data needs to take account of the stress dependency as well as the strain dependency. Unlike the undrained case, the mean effective stress increases during a drained cavity expansion so the

coincidence of stiffness data seen in Fig. 16 no longer applies. Fig. 20 is an example, using data from the unload/reload cycles shown in Fig. 18.

There are techniques that allow the stiffness response at a specific value of mean effective stress to be identified (for example Bellotti et al, 1989). Generally the first cycle in a test such as that in Fig. 18 is likely to be reasonably close to the value at the first yield state.

5.1. Drained equations for curve modelling

The following equations follow the same format as the undrained case. Plastic expansion in a c′- ϕ′ material:

$$P'_c = (P'_f + c' \cot \phi') \left[\frac{\varepsilon_c}{\varepsilon_{ip}(1+\sin\psi)} + \left(\frac{\sin\psi}{(1+\sin\psi)}\right)\right]^S - c' \cot \phi' \quad (10)$$

P'_f and ε_{ip} are the effective radial stress and cavity strain at first yield. For a material with a non-linear response prior to yield they are defined as follows:

$$P'_c = P'_f = P'_o + \left(\frac{(p'_o \sin\phi + c' \cos\phi)}{\beta(1+\sin\phi) - \sin\phi}\right) \quad (11)$$

$$\varepsilon_{ip} = \left(\frac{P'_f - P'_o}{\alpha_r}\right)^{\frac{1}{\beta}} \quad (12)$$

The curve modelling is in radial stress/cavity strain space and the stiffness data needs to be adapted to suit. α_r is calculated from the shear stress constant α:

$$\alpha_r = 10^{\left(\log\frac{\alpha}{\beta} + \beta \log 2\right)} \quad (13)$$

It follows that below yield, the effective radial stress at the cavity wall is given by:

$$P'_c = P'_0 + \alpha_r (\varepsilon_c)^\beta \quad (14)$$

Perfectly plastic contraction, incorporating drained cohesion, is given by:

$$P'_c = (P'_{fu} + c' \cot \phi') \left[A_c \left(\frac{\varepsilon_{mx} - \varepsilon_c}{\varepsilon_{ipu}}\right) - B_c\right]^{s_{ul}} - c' \cot \phi' \quad (15)$$

A_c and B_c are two constants defined in Table 1. p'_{fu} and ε_{ipu} are the yield stress and strain in contraction. The non-linear sub-yield response is :

$$P'_c = P'_{mx} - \alpha_{ru} (\varepsilon_{mx} - \varepsilon_c)^\beta \quad (16)$$

This applies until yield in contraction:

$$P'_c = P'_{fu} = P'_{mx} - \left(\frac{2(P'_{mx} \sin\phi - c' \cos\phi)}{\beta(1-\sin\phi) + 2\sin\phi}\right) \quad (17)$$

The cavity strain at the yield state will be:

$$\varepsilon_c = \varepsilon_{ipu} = \varepsilon_{mx} - \left(\frac{P'_{mx} - P'_{fu}}{\alpha_{ru}}\right)^{\frac{1}{\beta}} \quad (18)$$

If the material deformation is purely frictional and the response is linear elastic up to yield then all these equations revert to published solutions. Equation (10) can be derived from Hughes et al (1977) and equ. (15) becomes that of Withers et al (1989).

Fig.21 is an example of the model used in a medium dense sand without cohesion. This is the same test shown in Fig. 19 and Fig. 20.

Fig. 22 is an example of a test conducted in a tailings dam. The results indicate that the material has a small amount of cohesion and because it lies close to the critical state is *potentially* liquefiable.

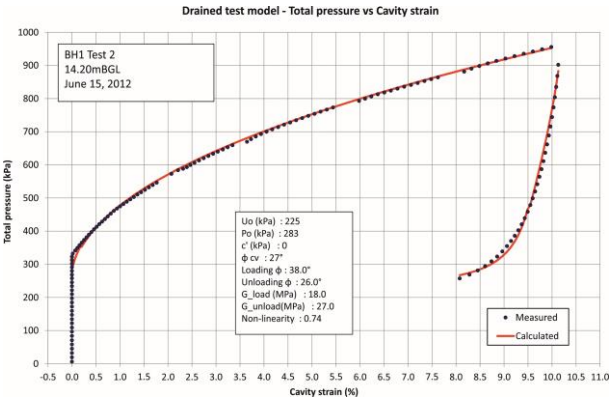

Figure 21. The sand model (purely frictional)

5.2. Determining the drained shear modulus at yield

The drained curve model (Fig. 21 and Fig. 22) uses two values for shear modulus, applicable to the first yield and yield when the cavity is contracting. What is required from the unload/reload cycles is a description of how shear modulus develops with strain and stress level.

The cycles are initiated at a measured value of effective radial stress at the cavity wall, P'_c. This is converted to mean effective stress σ'_{av} by the following:

$$\sigma'_{av} = P'_c / (1 + \sin\phi') \quad (19)$$

Here, ϕ' is the peak angle of internal friction decided by use of the Hughes et al 1977 analysis (Fig. 19). There are more sophisticated versions of equ. (19) but for the purposes of the model, it is sufficient.

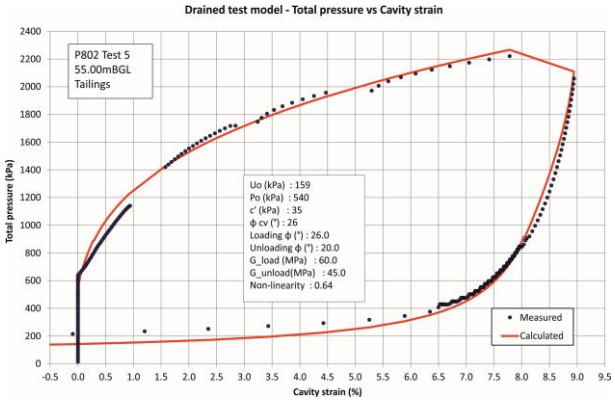

Figure 22. The drained model, friction and cohesion

Each cycle produces a pair of α and β parameters. Select a value of shear strain (0.3% is the model default value) then plot the resulting secant shear modulus against σ'_{av}. Fig. 23 is an example, for three strain levels. Usually it is necessary to use log scales to linearize the data but for this example linear scales give the best correlation coefficients.

Fig. 23 illustrates that for a given strain and stress, the shear modulus can be predicted from the unload/reload response. The particular values required for modelling are the mean effective stress and strain when the material reaches the yield condition, both in expansion and contraction. When the model is being used, the yield co-

ordinates will change and so the required shear modulus values will be re-calculated after every adjustment.

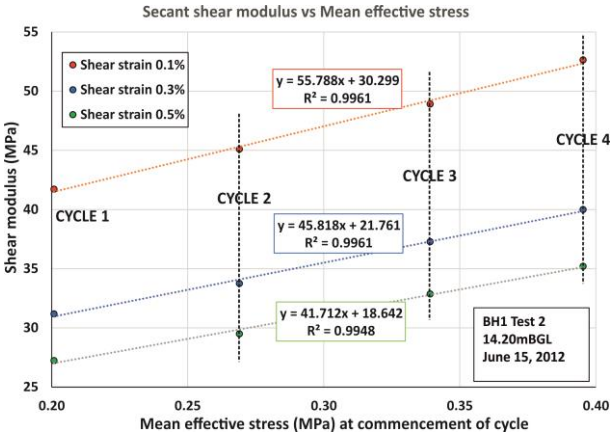

Figure 23. G_s variation with strain and stress

Each unload/reload cycle can only give one value for the relevant mean effective stress. The drained test shown in Fig. 18 has 4 cycles to give the stiffness-stress derivations a reasonable level of credibility. For the undrained case, 2 cycles would be sufficient.

The process is slightly simplified for the contraction; provided that the stress reductions are within the sub-yield range, the value of mean effective stress is that which existed at the moment the cavity contraction began. Therefore it is only necessary to find the cavity contraction yield strain in order to calculate the required shear modulus.

5.3. Using creep data to identify P_o.

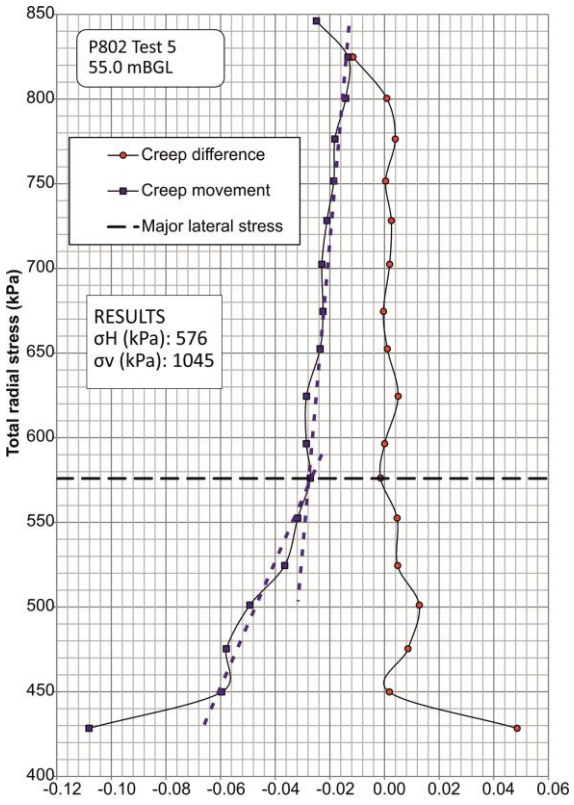

Figure 24. Cavity contraction creep

Hoopes and Hughes (2013) suggest that creep displacement readings taken during the cavity contraction phase of the test may indicate the cavity reference pressure P_0. Their paper was concerned with undrained tests in clay but a similar argument can be made for drained tests.

The concept is that creep displacements will be a minimum when the pressure applied at the cavity wall matches the geostatic stress. In Fig. 22 the part of the final contraction between 900 and 400 kPa consists of small decrements of pressure, each held for 1 minute. Fig. 24 plots the results as an absolute displacement and as a difference between successive steps. In this example it is the absolute movement that shows a clear deviation at 576kPa. This is slightly more than the P_0 derived from the drained modelling (Fig. 22) but is within 7%. The importance of this approach to determining P_0 and by inference σ_{ho} is that the cavity contraction phase of the test is independent of the probe insertion method, and hence a pre-bored or pushed pressuremeter is able to make reasonable estimates comparable with the self-boring method. However the movements are very small so the ability to resolve micrometre changes is a pre-requisite.

5.4. Limitations of the drained model

As with the undrained solution the greatest weakness of the model is the assumption of perfect plasticity. This is a particular difficulty with cavity contraction data, and so the model allows for the loading and contraction phase to have different angles of peak friction. This introduces a degree of freedom (and therefore uncertainty) in its application.

Drained cohesion cannot be separately quantified by the analysis methods available, so it is an additional free parameter. However as the same value affects the loading and contraction phases of the test, identifying inappropriate cohesion parameters is not difficult.

For both models the one fixed parameter is stiffness. Because for the drained case stiffness is stress as well as strain dependent, the software that implements the model uses an iterative approach. When the strength components of the calculated curve are altered this changes the mean effective stress at yield and the pertinent shear modulus is then recalculated. Accurate calculation depends on having several unload/reload cycles from the one test to evaluate.

6. Concluding remarks

The purpose of this paper is to show how relatively simple but rigorous solutions for the cavity expansion test can be used to convert pressuremeter field curves to fundamental soil parameters. No pressuremeter specific parameters or empirical correlations are required. The data approached in this way uses the same engineering terminology and concepts as laboratory testing or finite element analysis.

Confidence in the analysis process is achieved by showing how a set of parameters initially obtained by analysis recovers the measured field curve.

Other solutions and approaches are available, and have been for some time. Ferreira and Robertson (1992), for example, give an undrained solution based on a hyperbolic stiffness degradation that requires the small

strain shear modulus to be known. The primary advantage of the approach presented in this paper is the certainty of knowing the shear modulus at yield, and then working back to stiffness at smaller strains.

Most of the examples are taken from self-bored tests but much of the methodology can be applied to more invasive techniques provided that high quality data are available for the sub-yield response of the ground obtained from unload/reload cycles.

Unquestionably these methods are harder to apply than the Ménard method. The reward for persevering is a rich understanding of the nature of the ground, unlocking the predictive potential of the cavity expansion test. Figure 25 illustrates the difference. The MPM data are taken from Gibson & Anderson (1961). The SBP data are from the same location some years later.

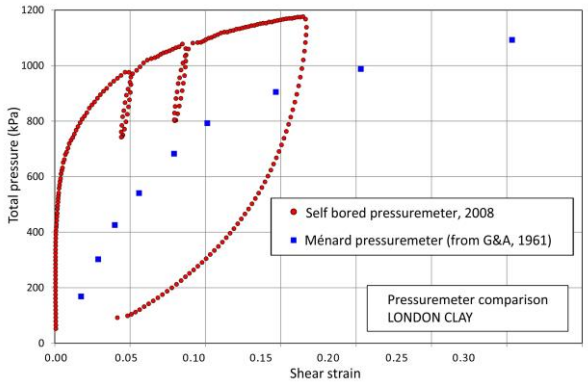

Figure 25. MPM and SBP compared

As far as strength is concerned, the two tests are showing similar results. The major difference is the absence of any sub-yield data in the MPM test. This is why the SBP remains such a powerful investigative tool.

Acknowledgements

The Authors have taken some material, images and the general approach from:

Hughes, John and Whittle, Robert. 2023. "High Resolution Pressuremeters and Geotechnical Engineering. The Measurement of Small Things". Publ. Taylor & Francis Ltd, ISBN: 9781032060941

References

Bellotti, R., Ghionna, V., Jamiolkowski, M., Robertson, P. and Peterson, R. 1989. "Interpretation of moduli from self-boring pressuremeter tests in sand." *Géotechnique* **39** (2), pp.269 - 292.

Bishop, R.F., Hill, R. and Mott, N.F . 1945. "The theory of indentation and hardness tests". Proc. Phys. Soc. Vol. 57, No.3, p 167.

Bolton M.D. and Whittle R.W. 1999. "A non-linear elastic/perfectly plastic analysis for plane strain undrained expansion tests." *Géotechnique* Vol. 49, No.1, pp 133-141.

Carter, J.P., Booker, J.P., and Yeung, S.K. 1986. "Cavity expansion in cohesive frictional soils". *Géotechnique* **36** (3), pp. 349-358.

Ferreira, R. S. and Robertson, P. K. 1992**. "**Interpretation of undrained self-boring pressuremeter test results incorporating unloading." Can. Geotech., **29**, pp 918--928.

Gibson, R.E. and Anderson, W.F. 1961. "In situ measurement of soil properties with the pressuremeter", Civil Engineering and Public Works Review, Vol. 56, No. 658 May pp. 615-618.

Hoopes, O and Hughes, J.M.O. 2014. "In situ Lateral Stress Measurement in Glaciolacustrine Seattle Clay Using the Pressuremeter" . J. of Geotechnical and Geoenvironmental Engineering, **140** (5).

Houlsby, G.T., Clarke B.G. and Wroth P.C. 1986. "Analysis of the unloading of a pressuremeter test in sand". *The Pressuremeter and its Marine Applications: 2nd .Int. Symp.,* pp. 245-262.

Houlsby, G. and Withers, N.J. 1988. "Analysis of the Cone Pressuremeter Test in Clay." *Géotechnique*, **38** (4), pages 573-587.

Hughes, J.M.O., Wroth, C.P. and Windle, D. 1977. "Pressuremeter tests in sands". *Géotechnique* **27** (4), pp. 455-498.

Jefferies, M.G. 1988. "Determination of horizontal geostatic stress in clay with self-bored pressuremeter." Can. Geotech. 25 (3), pp 559-573.

Palmer, A.C. 1972. "Undrained plane-strain expansion of a cylindrical cavity in clay: a simple interpretation of the pressuremeter test." *Géotechnique* **22** (3) pp 451-457.

Manassero, M. 1989. "Stress-strain relationships from drained self-boring pressuremeter tests in sands." *Géotechnique*, **39** (2): pp 293-307.

Rowe, P.W. 1962. "The Stress Dilatancy Relation for Static Equilibrium of an Assembly of Particles in Contact." *Proc. of the Royal Society*. Vol. 269, Series A, pp 500-527.

Whittle R.W. 1999. "Using non-linear elasticity to obtain the engineering properties of clay." Ground Engineering, May, vol. 32, no.5, pp 30-34.

Whittle, R.W and Byrne, Y. 2020. "Deriving stress/strain relationships from the contraction phase of pressuremeter tests in sands." Proc. Geovirtual 2020, Calgary, Canada, 14-16 Sept, Paper 107.

Table 1. Nomenclature

Symbols	Description
c_u	Undrained shear strength
c'	is drained cohesion
G_{ye}	Secant shear modulus at first yield (expansion)
G_{yc}	Secant shear modulus at yield in contraction
P	Total pressure (radial stress at the cavity wall)
P_c'	is effective pressure at the cavity wall
P_o	is cavity reference pressure .
P_o'	is effective cavity reference pressure .
P_L	Total limit pressure for indefinite expansion
P_{LM}	Ménard limit pressure ($= P_L - c_u \ln 2$)
P_{mx}	Maximum expansion pressure at the end of loading.
P'_{mx}	is the effective maximum expansion pressure
P_f'	Effective radial at the cavity wall when first yielding
P_{fu}'	Effective radial at the cavity wall when yielding in contraction
σ	Stress. σ_{ho} is the insitu horizontal stress.
γ	Shear strain
γ_{cc}	Shear strain in contraction
γ_{yc}	Shear strain at yield in contraction
γ_{ye}	Shear strain at first yield
A	Area. ΔA/A is constant area ratio and is shear strain.
α	Shear stress constant. α_r and α_{ru} are *radial* stress constants for loading and unloading respectively (drained tests).
β	Exponent of non-linearity, typically between 0.5 and 1.

η	Radial stress intercept in radial stress/shear strain space.
V	Volume.
V_s	Volume at the cavity origin.
V_1, V_2	Volume at start and finish of pseudo-elastic phase.
P_1, P_2	Pressure at start and finish of pseudo-elastic phase
E	Young's modulus.
E_M	Ménard modulus
ε	Strain – subscript c is cavity strain
ε_{ip}	is circumferential yield strain when expanding
ε_{ipu}	is circumferential yield strain when contracting
ε_{mx}	is the maximum cavity strain at the end of loading
τ	Shear stress
S	Exponent of the drained plastic loading response. $S = \frac{(1+\sin\psi)\sin\phi'}{1+\sin\phi'}$
S_{ul}	Exponent of the drained plastic contraction response. $S_{ul} = \frac{-2\sin\phi'(1-\sin\psi)}{(1-\sin\phi')(1+\sin\phi'\sin\psi)}$
ν	is Poisson's ratio
ϕ'	is angle of shearing resistance.
ϕ'_{cv}	is the friction angle when the material is shearing at constant volume.
ψ	is dilation angle.
M	is $\frac{(1+sin\psi)}{(1-sin\psi)}$
N	is $\frac{(1+sin\phi)}{(1-sin\phi)}$
A_c	$A_c = (NM+1)/(N+1)$
B_c	$B_c = (NM-N)/(N+1)$